

\$Revision: 2.6 \$Date: 2013/12/02 15:32:54 , accepted to MNRAS

Bayesian Lensing Shear Measurement

Gary M. Bernstein

`garyb@physics.upenn.edu`

and

Robert Armstrong

`rearmstr@gmail.com`

Department of Physics & Astronomy, University of Pennsylvania, 209 S. 33rd St., Philadelphia, PA 19104

ABSTRACT

We derive an estimator of weak gravitational lensing shear from background galaxy images that avoids noise-induced biases through a rigorous Bayesian treatment of the measurement. The derived shear estimator dispenses with the assignment of ellipticities to individual galaxies that is typical of previous approaches to galaxy lensing. Shear estimates from the mean of the Bayesian posterior are unbiased in the limit of large number of background galaxies, regardless of the noise level on individual galaxies. The Bayesian formalism requires a prior describing the (noiseless) distribution of the target galaxy population over some parameter space; this prior can be constructed from low-noise images of a subsample of the target population, attainable from long integrations of a fraction of the survey field. We find two ways to combine this exact treatment of noise with rigorous treatment of the effects of the instrumental point-spread function and sampling. The Bayesian model fitting (BMF) method assigns a likelihood of the pixel data to galaxy models (e.g. Sersic ellipses), and requires the unlensed distribution of galaxies over the model parameters as a prior. The Bayesian Fourier domain (BFD) method compresses the pixel data to a small set of weighted moments calculated after PSF correction in Fourier space. It requires the unlensed distribution of galaxy moments as a prior, plus derivatives of this prior under applied shear. A numerical test using a simplified model of a biased galaxy measurement process demonstrates that the Bayesian formalism recovers applied shears to < 1 part in 10^3 accuracy as well as providing accurate uncertainty estimates. BFD is the first shear measurement algorithm that is model-free and requires no approximations or *ad hoc* assumptions in correcting for the effects of PSF, noise, or sampling on the galaxy images. These algorithms are good

candidates for attaining the part-per-thousand shear inference required for hemisphere-scale weak gravitational lensing surveys. BMF has the drawback that shear biases will occur since galaxies do not fit any finite-parameter model, but has the advantage of being robust to missing data or non-stationary noise. Both BMF and BFD methods are readily extended to use data from multiple exposures and to inference of lensing magnification.

Subject headings: gravitational lensing: weak—methods: data analysis

1. Introduction

Gravitational lensing reveals the mass distribution of the Universe by detecting deflections of photons in the gravitational potential generated by the mass. Along most lines of sight, we can best measure the *gradient* of the deflection, characterized by an apparent shear \mathbf{g} and magnification of background sources.¹ The lensing shear is detectable as a coherent alignment induced on nominally randomly-oriented resolved background galaxies. Reliable measurement of this shear opens the door to a wealth of astrophysical and cosmological information, including the most direct measures of the dark components of the Universe. See Hoekstra & Jain (2008) and Weinberg et al. (2013) for recent reviews of the power of this weak gravitational lensing technique.

The full power of the weak lensing technique can only be realized, however, if we are able to infer the shear from real image data without significant systematic error. This apparently straightforward measurement is complicated by several factors:

- The shear is weak, amounting to $\approx 2\%$ change in a galaxy’s axis ratio on a typical cosmological line of sight. In a full-sky experiment, it is possible to measure shear with statistical errors below 1 part in 10^3 of this 2%—systematic errors must be extremely small else they will dominate the error budget.
- The galaxy is viewed through an instrument (possibly including the atmosphere) which convolves the lensed appearance with a point spread function (PSF) that typically induces larger coherent shape changes than the gravitational lensing, and can vary with time and with position on the sky. This instrumental effect must be known and removed.
- The received image of the galaxy is pixelized, meaning it has finite sampling. Even if the sampling meets the Nyquist criterion so that the image is unambiguous, our shear extraction algorithm must handle the sampling and any other signatures of the detector.

¹There are several possible parameterizations for the gradient matrix in terms of shear. We will leave this unspecified to emphasize that our method is valid for any choice of parameterization.

- The unlensed appearance of any individual galaxy is unknown, and galaxies have an infinite variety of intrinsic shapes. No finite parameterization can fully describe the unlensed galaxies.
- The received image includes photon shot noise and additional noise from the detector. The shear inference must maintain exceptionally low bias even when targeting galaxies with signal-to-noise ratio $S/N < 10$ –15 if we are to extract the bulk of the shear information available from typical optical sky images.

Heymans et al. (2006), Massey et al. (2007), Bridle et al. (2010), and Kitching et al. (2012) document a series of challenges in which the community was invited to infer the shear from simulated sky images, as a means of assessing our abilities to measure shear in the face of the above difficulties. These publications also summarize the impressive variety of techniques that have been proposed for shear inference. A useful parameterization for errors in shear inference is (using a simplified scalar notation) that the measured shear \hat{g} is related to the true shear via

$$\hat{g} = (1 + m)g + c. \quad (1)$$

Huterer et al. (2006) calculate that ambitious weak-shear surveys must obtain multiplicative errors $|m| < 10^{-3}$ to retain their full statistical power. The additive bias c , which can arise when the PSF or other element of the analysis chain is not symmetric under 90° rotation, must be kept below $\approx 10^{-3.5}$, which is 100–300 \times smaller than the typical PSF ellipticity. The literature contains no demonstrations of robust shear algorithms yielding $|m| < 0.01$ at $S/N \approx 10$.

Bernstein (2010) demonstrates the ability to attain $|m| < 10^{-3}$ at high S/N , overcoming all but the last of the problems itemized above. This “FDNT” method has a rigorous formulation for noiseless data. It has, however, proven more difficult to derive a shear inference that is rigorously correct in the presence of noise. Refregier et al. (2012) derive the lowest-order noise-induced bias in galaxy-shape estimates that are produced via maximum-likelihood fitting to parametric galaxy models. But it is not clear that this correction yields the necessary accuracy on real data. The most common approach to biases induced by noise (or other systematic errors) has been to use simulated sky data to infer m and then apply a correction to the real-sky result. The accuracy of this approach is of course limited by the extent to which the simulated data reproduces the salient characteristics of the real sky. Kacprzak et al. (2012) propose a somewhat more general scheme of calibrating shape-measurement biases vs a few parameters of the galaxy and measurement, *e.g.* the S/N level, resolution, Sersic index, etc., and then applying bias corrections on a galaxy-by-galaxy basis. But Zuntz et al. (2013) note that this galaxy-by-galaxy bias correction is inaccurate at low S/N , and it is better to determine a single overall correction to the shear using prior high- S/N information on a random subsample of the source population.

All these avenues lead us back to the situation of requiring prior empirical high- S/N information on the underlying source galaxy population in order to produce the noise-bias corrections. Once we need an empirical prior on galaxy information, we should look to Bayesian techniques to produce a rigorously correct shear estimator. The LENSFIT method of Miller et al. (2007, LENSFIT)

produces a Bayesian posterior distribution $P(\mathbf{e}_i|\mathbf{D}_i)$ for the ellipticity of galaxy i given its pixel data \mathbf{D}_i , assuming that galaxies take a known functional form and given a prior distribution of \mathbf{e} and the other parameters of the presumed galaxy model. But in LENSFIT the inference of applied shear \mathbf{g} from an ensemble of these posterior densities for galaxy shapes is done using some *ad hoc* weighting and averaging schemes. Testing of the LENSFIT codes on simulated data in Miller et al. (2013) yields $|m| \sim 0.1$ at $S/N = 10$, necessitating an empirical multiplicative correction to shears derived from real data.

In this paper we will derive a rigorous Bayesian treatment of the inference of weak shear, not just galaxy shapes, from pixel data. The general approach is outlined in Section 2. Then we examine three ways to apply this approach to real data: Section 3 examines Bayesian model-fitting (BMF) approaches and extends the LENSFIT Bayesian method to shear estimation. Section 4 then shows how to apply Bayesian techniques without assuming a parametric model for unlensed galaxies, yielding an adaptation of the venerable Kaiser et al. (1995, KSB) weighted-moment method that treats convolution, sampling, and noise rigorously. We consider this Bayesian Fourier-domain (BFD) method to be our most promising algorithm for high-accuracy shear inference. In Section 5 we explore whether the FDNT method that is successful at high S/N can be embedded in a Bayesian framework for accuracy at finite S/N . In Sections 6 and 7 we compare to some extant shear-measurement algorithms and conclude.

2. Bayesian shear estimate

2.1. General formulation

We begin by assuming that we wish to infer the posterior distribution of a constant shear \mathbf{g} from an image containing data \mathbf{D} that can be subdivided into statistically independent subsets \mathbf{D}_i , each covering a single galaxy $i \in \{1, \dots, N_g\}$. For a prior probability $P(\mathbf{g})$ of the shear, the standard Bayesian formulation for the posterior is

$$P(\mathbf{g}|\mathbf{D}) = \frac{P(\mathbf{g})P(\mathbf{D}|\mathbf{g})}{P(\mathbf{D})} = P(\mathbf{g}) \prod_i \frac{P(\mathbf{D}_i|\mathbf{g})}{P(\mathbf{D}_i)}. \quad (2)$$

Our fundamental assumption is that the posterior $\ln P(\mathbf{g}|\mathbf{D})$ will be well approximated by a quadratic Taylor expansion in \mathbf{g} , *i.e.* the posterior will be Gaussian in \mathbf{g} . This assumption will fail when the number of galaxies is small and the shear is poorly constrained, but should become valid when we combine information from a large number of galaxies on a weak shear. In Appendix A we give a prescription for including 3rd-order terms in \mathbf{g} as perturbations, since terms $O(g^3)$ are necessary if the estimate of \mathbf{g} is to be accurate to < 1 part in 10^{-3} for $g \approx 0.03$.

The Bayesian formulation (2) produces an exact posterior distribution of the shear. The full posterior distribution could be propagated into cosmological inferences, but most current analyses require instead an estimator \hat{g} for the shear (and an uncertainty). By adopting a quadratic Taylor

expansion for $\ln P(\mathbf{g}|\mathbf{D})$ we implicitly assume that the maximum of the posterior distribution is coincident with the mean of the posterior, so it would be natural to adopt the location $\bar{\mathbf{g}}$ of this posterior peak as a shear estimator. Below we will consider whether this estimate is biased.

For quadratic order, we need the 6 scalars that make up the scalar P_i , vector \mathbf{Q}_i , and symmetric 2×2 matrix \mathbf{R}_i defined as:

$$\begin{aligned} P_i &= P(\mathbf{D}_i|\mathbf{g}=0) \\ \mathbf{Q}_i &= \nabla_{\mathbf{g}} P(\mathbf{D}_i|\mathbf{g})|_{\mathbf{g}=0} \end{aligned} \quad (3)$$

$$\begin{aligned} \mathbf{R}_i &= \nabla_{\mathbf{g}} \nabla_{\mathbf{g}} P(\mathbf{D}_i|\mathbf{g})|_{\mathbf{g}=0} \\ \Rightarrow P(\mathbf{D}_i|\mathbf{g}) &\approx P_i + \mathbf{g} \cdot \mathbf{Q}_i + \frac{1}{2} \mathbf{g} \cdot \mathbf{R}_i \cdot \mathbf{g}. \end{aligned} \quad (4)$$

The dependence of the posterior on \mathbf{g} can now be expressed as

$$-\ln P(\mathbf{g}|\mathbf{D}) \approx (\text{const}) - \ln P(\mathbf{g}) - \mathbf{g} \cdot \sum_i \frac{\mathbf{Q}_i}{P_i} + \frac{1}{2} \mathbf{g} \cdot \left[\sum_i \left(\frac{\mathbf{Q}_i \mathbf{Q}_i^T}{P_i^2} - \frac{\mathbf{R}_i}{P_i} \right) \right] \cdot \mathbf{g}. \quad (5)$$

If we presume that the data are much more informative than the prior on \mathbf{g} , we may drop the $\ln P(\mathbf{g})$ and find that the posterior for the shear is Gaussian with covariance matrix \mathbf{C}_g and mean $\bar{\mathbf{g}}$ defined via

$$\mathbf{C}_g^{-1} = \sum_i \left(\frac{\mathbf{Q}_i \mathbf{Q}_i^T}{P_i^2} - \frac{\mathbf{R}_i}{P_i} \right) \quad (6)$$

$$\bar{\mathbf{g}} = \mathbf{C}_g \sum_i \frac{\mathbf{Q}_i}{P_i}. \quad (7)$$

Note that we have *not* made any assumption about the Gaussianity of the likelihood $P(\mathbf{D}_i|\mathbf{g})$ for each galaxy, nor about any priors, etc.; only about the posterior of the applied shear \mathbf{g} .

2.2. Non-constant shear

Before describing methods of calculating $P(\mathbf{D}_i|\mathbf{g})$ and its derivatives, we discuss generalization of (5) to non-constant shear fields. Once the quantities P_i , \mathbf{Q}_i , and \mathbf{R}_i are calculated for each galaxy, the posterior for any shear model can be calculated as long as the model predicts shears in the regime where (4) holds. Consider a model with parameter vector \mathbf{a} which predicts shear values $\mathbf{g}_i(\mathbf{a})$ at each galaxy. We can slightly modify our formulation and proceed as before to derive the posterior $P(\mathbf{a}|\mathbf{D})$

$$-\ln P(\mathbf{a}|\mathbf{D}) \approx (\text{const}) - \ln P(\mathbf{a}) - \sum_i \mathbf{g}_i(\mathbf{a}) \cdot \frac{\mathbf{Q}_i}{P_i} + \frac{1}{2} \sum_i \mathbf{g}_i(\mathbf{a}) \cdot \left[\sum_i \left(\frac{\mathbf{Q}_i \mathbf{Q}_i^T}{P_i^2} - \frac{\mathbf{R}_i}{P_i} \right) \right] \cdot \mathbf{g}_i(\mathbf{a}), \quad (8)$$

If \mathbf{g} is a linear function of \mathbf{a} (and if the prior is approximated as quadratic), then the solution for the maximum-posterior \mathbf{a} is a closed-form matrix equation. One potentially interesting application is a Fourier decomposition $\mathbf{g}_i = \sum_{\mu} \text{Re}(\mathbf{a}_{\mu} e^{i\mathbf{k}_{\mu} \cdot \mathbf{x}_i})$. If the source galaxies are uniformly distributed on the plane and we can make the approximation that

$$\sum_i \left(\frac{\mathbf{Q}_i \mathbf{Q}_i^T}{P_i^2} - \frac{\mathbf{R}_i}{P_i} \right) e^{i\mathbf{k} \cdot \mathbf{x}_i} = 0 \quad \text{for } \mathbf{k} \neq 0, \quad (9)$$

then dependence of the posterior on the Fourier coefficients becomes

$$\begin{aligned} \ln P(\mathbf{a}|\mathbf{D}) \approx & \sum_{\mu} \text{Re} \left[\mathbf{a}_{\mu} \sum_i \frac{\mathbf{Q}_i}{P_i} e^{i\mathbf{k}_{\mu} \cdot \mathbf{x}_i} \right] \\ & + \frac{1}{4} \sum_{\mu} \mathbf{a}_{\mu} \cdot \mathbf{C}_g^{-1} \cdot \mathbf{a}_{\mu}^*, \end{aligned} \quad (10)$$

with \mathbf{C}_g^{-1} as from (6). This posterior separates into a Gaussian over each 2-component \mathbf{a}_{μ} with identical covariance $2\mathbf{C}_g^{-1}$ on each of the real and imaginary parts of each Fourier coefficient and a simple 2×2 matrix solution for the most probable \mathbf{a}_{μ} . A similarly simple posterior could be derived for any decomposition of the shear field into orthogonal functions.

Bayesian estimation of N -point correlations of a shear field should also be similarly straightforward, at least in the limit where galaxy shape noise and measurement noise are dominant over the sample variance of the shear field. We leave this derivation for future work.

2.3. Bias of the Bayesian posterior

Is the mean $\bar{\mathbf{g}}$ from Equation (7) an unbiased estimator of the true shear \mathbf{g} ? The Bayes formalism does not guarantee that the mean of the posterior is an unbiased estimator. It does assure, however that the posterior $P(\mathbf{g}|\mathbf{D})$ converges to the input value if the posterior is narrow, *i.e.* the Bayesian posterior is not *wrong*.

Define $\bar{\mathbf{b}} = \langle \mathbf{Q}_i / P_i \rangle$ as the expectation of the summand in Equation (7) over the population of target galaxies, and define

$$\bar{\mathbf{A}} = \langle \mathbf{A}_i \rangle = \left\langle \frac{\mathbf{Q}_i \mathbf{Q}_i^T}{P_i^2} - \frac{\mathbf{R}_i}{P_i} \right\rangle. \quad (11)$$

For each galaxy we can define $\delta \mathbf{A}_i = \mathbf{A}_i - \bar{\mathbf{A}}$ and $\delta \mathbf{b}_i = \mathbf{Q}_i / P_i - \bar{\mathbf{b}}$.

When we ignore the prior $P(\mathbf{g})$ as weakly informative relative to the data from a large number

N of galaxies, the expectation of the mean $\bar{\mathbf{g}}$ of the posterior $P(\mathbf{g}|\mathbf{D})$ in Equation (7) becomes

$$\langle \bar{\mathbf{g}} \rangle = \left\langle \left(N\bar{\mathbf{A}} + \sum \delta\mathbf{A}_i \right)^{-1} \left(N\bar{\mathbf{b}} + \sum \delta\mathbf{b}_i \right) \right\rangle \quad (12)$$

$$= \left\langle \left(N\bar{\mathbf{A}} \right)^{-1} \left(\mathbf{I} + \frac{1}{N} \sum \mathbf{A}^{-1} \delta\mathbf{A}_i \right)^{-1} \left(N\bar{\mathbf{b}} + \sum \delta\mathbf{b}_i \right) \right\rangle \quad (13)$$

$$= \bar{\mathbf{A}}^{-1} \bar{\mathbf{b}} + \frac{1}{N} \bar{\mathbf{A}}^{-1} \left[\left\langle \delta\mathbf{A} \bar{\mathbf{A}}^{-1} \delta\mathbf{A} \right\rangle \bar{\mathbf{A}}^{-1} \bar{\mathbf{b}} - \left\langle \delta\mathbf{A} \bar{\mathbf{A}}^{-1} \delta\mathbf{b} \right\rangle \right] + O(N^{-2}). \quad (14)$$

The last line arises from expanding $(\mathbf{I} + \mathbf{M})^{-1} \approx \mathbf{I} - \mathbf{M} + \mathbf{M}\mathbf{M} - \dots$, and using $\langle \delta\mathbf{b} \rangle = 0$, $\langle \delta\mathbf{A} \rangle = 0$.

As $N \rightarrow \infty$, $\mathbf{C}_g \rightarrow (N\bar{\mathbf{A}})^{-1}$ and the posterior narrows to a delta function at $\bar{\mathbf{g}}_\infty = \bar{\mathbf{A}}^{-1} \bar{\mathbf{b}}$. To the extent that our quadratic approximation is valid, Bayes theorem demands that this equal the true input \mathbf{g} . We find then that the bias for a finite set of galaxy is, to leading order in $1/N$,

$$\langle \bar{\mathbf{g}} \rangle - \mathbf{g} \approx \frac{1}{N} \bar{\mathbf{A}}^{-1} \left[\left\langle \delta\mathbf{A} \bar{\mathbf{A}}^{-1} \delta\mathbf{A} \right\rangle \mathbf{g} - \left\langle \delta\mathbf{A} \bar{\mathbf{A}}^{-1} \delta\mathbf{b} \right\rangle \right]. \quad (15)$$

The first bracketed term is roughly a multiplicative bias (not quite, because the distributions of \mathbf{A} will depend weakly on \mathbf{g}). If we have $\bar{\mathbf{A}}^{-1} \delta\mathbf{A} = O(1)$, then this multiplicative bias on shear is $O(1/N)$. This bias will be $\sim \sqrt{N}$ smaller than the statistical error $\sigma_g/\sqrt{N} \approx 0.3/\sqrt{N}$ that arises from shape noise in a weak lensing measurement.

The forms of \mathbf{b} and \mathbf{A} suggest that $(\delta\mathbf{b})^2 \sim \bar{\mathbf{A}} \sim \sigma_g^{-2}$ in magnitude, so the second term can be expected to scale as σ_g/N . In addition, this term involving covariance between \mathbf{A} and \mathbf{b} will vanish by symmetry at $\mathbf{g} = 0$ if the PSF and noise are isotropic. Therefore we expect this bias to have another factor of g or of e_\star , the PSF ellipticity, in front of it, leading to an additive bias of perhaps $e_\star \sigma_g/N$. This will again always be below shape noise and insignificant for shear statistics constrained by $N \gg 10^4$ galaxy measurements.

These terms do represent a kind of noise bias on the mean of the shear posterior taken as a shear estimator. The principal difference from previous techniques, however, is that the size of this bias scales as the square of the measurement error on the *shear*, and is not affected by measurement errors on individual galaxy shapes.

2.4. Galaxy descriptors

Implementation of the Bayesian method depends on assigning a probability $P(\mathbf{D}_i|\mathbf{g})$ to the pixel data given the shear. To do so we introduce some finite set \mathbf{G}_i of quantities describing the appearance of galaxy i . We must be able to assign a likelihood $\mathcal{L}(\mathbf{D}|\mathbf{G})$ of the pixel data \mathbf{D} being produced by a galaxy with properties \mathbf{G} . We also need to know the distribution of \mathbf{G} for the true galaxy population viewed through shear \mathbf{g} . Then we can assign

$$P(\mathbf{D}_i|\mathbf{g}) = \int d\mathbf{G} \mathcal{L}(\mathbf{D}_i|\mathbf{G}) P(\mathbf{G}|\mathbf{g}). \quad (16)$$

The derivatives with respect to \mathbf{g} needed to define \mathbf{Q}_i , and \mathbf{R}_i in (3) all propagate purely to the prior $P(\mathbf{G}|\mathbf{g})$ inside the integral.

In the next two sections, we will consider first a model-fitting approach, in which the galaxy properties \mathbf{G} are assumed to predict all of the observed pixel data values; and a model-free scheme, in which the pixel data are compressed to a smaller set \mathbf{M} of moments that will serve as our galaxy properties. In either case, the essential requirements are that:

1. We have a rigorous means to assign a likelihood $\mathcal{L}(\mathbf{D}|\mathbf{G})$, and
2. The distribution of real galaxies' properties \mathbf{G} changes under application of shear \mathbf{g} , and that we can determine this dependence $P(\mathbf{D}|\mathbf{g})$ —*i.e.* there is a detectable and known signature of shear upon the galaxy population.

3. $P(\mathbf{D}_i|\mathbf{g})$ via model fitting

3.1. General Formulation

If galaxy i is assumed to be fully described by a model with a finite number of parameters \mathbf{G} , all the instrumental signatures are known, and there is a known noise model for the pixel data, then one can calculate the likelihood of the full pixel data vector $\mathcal{L}(\mathbf{D}_i|\mathbf{e}_i^o, \mathbf{x}_i, \boldsymbol{\theta}_i)$. Here we divide \mathbf{G} into three subsets:

- \mathbf{e}_i^o is a vector of observed parameters that are altered under the action of lensing shear \mathbf{g} , *i.e.* the ellipticity of the galaxy model. We presume that there is an exactly known transformation under the action of shear from intrinsic source parameters to the observed parameters, $\mathbf{e}^o = \mathbf{e}^s \oplus \mathbf{g}$. Such is the case, for example, when \mathbf{e} is the 2-component ellipticity of a galaxy with self-similar elliptical isophotes and \mathbf{g} is any of the common representations of the shear linear transformation matrix. We leave the form of this transformation free at this point to accommodate any convention for the definition of the ellipticity \mathbf{e} and the shear \mathbf{g} . We do, however, require that the transformation be reversible: $(\mathbf{e} \oplus \mathbf{g}) \oplus (-\mathbf{g}) = \mathbf{e}$.²
- \mathbf{x}_i is the center of the galaxy, or more generally any parameters whose prior distribution $P(\mathbf{x}_i)$ can be taken as uniform both before and after the application of shear to the sky. We hence will not make \mathbf{x}_i an argument of our priors.
- $\boldsymbol{\theta}_i$ are other parameters of the model, which we take to be invariant under the action of shear on the image. Examples would be the half-light radius, surface brightness, and Sersic index of a simple elliptical Sersic-profile galaxy model, *e.g.* as used in Miller et al. (2007).

² \mathbf{e} need not even be 2-dimensional: galaxy models with multiple components of different ellipticities might, for example, have 4 or more elements of \mathbf{e} . The key is that their transformation under shear must be known.

The shear-conditioned probability for single galaxy becomes

$$P(\mathbf{D}_i|\mathbf{g}) = \int de_i^o d\mathbf{x}_i d\boldsymbol{\theta}_i \mathcal{L}(\mathbf{D}_i|e_i^o, \mathbf{x}_i, \boldsymbol{\theta}_i) P(e_i^o, \boldsymbol{\theta}_i|\mathbf{g}), \quad (17)$$

where $P(e_i^o, \boldsymbol{\theta}_i|\mathbf{g})$ is the prior distribution the galaxy parameters given the shear. The shear enters the posterior only through this term. Conservation of probability under shear requires that

$$P(e^o, \boldsymbol{\theta}|\mathbf{g}) = P_0(e^o \oplus -\mathbf{g}, \boldsymbol{\theta}) \left| \frac{de^s}{de^o} \right|_{-\mathbf{g}}, \quad (18)$$

where $P_0(e, \boldsymbol{\theta})$ is the *unlensed* distribution of galaxy ellipticities, and the last term is the Jacobian of the ellipticity transformation $e^s = e^o \oplus -\mathbf{g}$. For an isotropic Universe, the unlensed prior should be a function only of the amplitude $e = |e|$, not the orientation. Given the unlensed prior, we can make a Taylor expansion in the shear:

$$P_0(e^o \oplus -\mathbf{g}, \boldsymbol{\theta}) \left| \frac{de^s}{de^o} \right|_{-\mathbf{g}} = P_0(e^o, \boldsymbol{\theta}) + \mathbf{g} \cdot \mathbf{Q}(e^o, \boldsymbol{\theta}) + \frac{1}{2} \mathbf{g} \cdot \mathbf{R}(e^o, \boldsymbol{\theta}) \cdot \mathbf{g} + O(g^3). \quad (19)$$

Once the transformation $e \oplus \mathbf{g}$ is specified, the functions \mathbf{Q} and \mathbf{R} can be derived in terms of $P_0(e, \boldsymbol{\theta})$ and its first two derivatives with respect to e . The quantities needed from each galaxy for the Bayesian posterior in Equation (5) are

$$\begin{Bmatrix} P_i \\ \mathbf{Q}_i \\ \mathbf{R}_i \end{Bmatrix} \equiv \int de_i^o d\mathbf{x}_i d\boldsymbol{\theta}_i \mathcal{L}(\mathbf{D}_i|e_i^o, \mathbf{x}_i, \boldsymbol{\theta}_i) \begin{Bmatrix} P_0(e_i^o, \boldsymbol{\theta}_i) \\ \mathbf{Q}(e_i^o, \boldsymbol{\theta}_i) \\ \mathbf{R}(e_i^o, \boldsymbol{\theta}_i) \end{Bmatrix}. \quad (20)$$

Note that P_i would be the Bayesian evidence for \mathbf{D}_i in the absence of lensing shear.

The operative procedure for obtaining the Bayesian shear estimate is:

1. Determine the unlensed prior $P_0(e, \boldsymbol{\theta})$ from a high- S/N imaging sample, and perform the Taylor expansion in Equation (19) knowing the ellipticity transformation equation.
2. For each observed galaxy, compute the six distinct integrals in (20) with the likelihood over the ellipticity and structural parameters to get P_i, \mathbf{Q}_i , and \mathbf{R}_i .
3. Sum over galaxies to obtain \mathbf{C}_g^{-1} in Equation (6).
4. Sum over galaxies to obtain the shear estimate $\bar{\mathbf{g}}$ as in Equation (7). The shear posterior has this mean (and maximum) and covariance matrix \mathbf{C}_g .

Note that the division by \mathbf{C}_g^{-1} occurs after the summation over galaxies, *i.e.* we do not generate ellipticity or shear estimators on a galaxy-by-galaxy basis. Also note that for galaxies with very noisy data, $\mathcal{L}(\mathbf{D}_i)$ is very weakly dependent on galaxy properties and hence on shear: $\nabla_{\mathbf{g}} P(\mathbf{D}_i|\mathbf{g}) \rightarrow 0$. Equations 3 then show that \mathbf{Q} and \mathbf{R} both tend to zero. The low- S/N galaxy hence has no

influence on the shear likelihood. It will therefore be unnecessary to make cuts on galaxy size or S/N ratio to obtain a successful measurement. As long as the source selection is made on a quantity (such as total flux) that is unaffected by galaxy shape or lensing shear, we avoid selection biases.

The only approximation made in this derivation was that of weak shear, namely that Equation (19) is accurate over the range of \mathbf{g} permitted by the data. If the unlensed ellipticity distribution is characterized by a scale of variation σ_e , this means we are assuming that $g \ll \sigma_e$.

Extension to multiple exposures of the same galaxy is trivial: the pixel data \mathbf{D}_i for galaxy i may be the union of N distinct exposures' information, $\mathbf{D}_i = \{\mathbf{D}_{i1}, \mathbf{D}_{i2}, \dots, \mathbf{D}_{iN}\}$. Assuming that different exposures have statistically independent errors, we have

$$\mathcal{L}(\mathbf{D}_i | \mathbf{e}_i^o, \mathbf{x}_i, \boldsymbol{\theta}_i) = \prod_{j=1}^N \mathcal{L}(\mathbf{D}_{ij} | \mathbf{e}_i^o, \mathbf{x}_i, \boldsymbol{\theta}_i). \quad (21)$$

If the exposures are in different filter bands, then the most general formulation is that \mathbf{e}_i and $\boldsymbol{\theta}_i$ are the unions of distinct structural parameters \mathbf{e}_{ij} and $\boldsymbol{\theta}_{ij}$ for each band j , and the prior must specify the joint distribution of galaxies' appearances in all observed bands.

An alternative formulation to the above is to integrate over the source ellipticity \mathbf{e}^s instead of the lensed ellipticity \mathbf{e}^o , which puts the derivatives with respect to shear in the likelihood instead of the prior:

$$P(\mathbf{D}_i | g) = \int d\mathbf{e}_i^s d\mathbf{x}_i d\boldsymbol{\theta}_i \mathcal{L}(\mathbf{D}_i | \mathbf{e}_i^s \oplus \mathbf{g}, \mathbf{x}_i, \boldsymbol{\theta}_i) P_0(\mathbf{e}_i^s, \boldsymbol{\theta}_i | \mathbf{g}). \quad (22)$$

In this case the quantities needed for the shear posterior are

$$\begin{aligned} P_i &\equiv \int d\mathbf{e}_i^s d\mathbf{x}_i d\boldsymbol{\theta}_i \mathcal{L}(\mathbf{D}_i | \mathbf{e}_i^s, \boldsymbol{\theta}_i) P_0(\mathbf{e}_i^s, \boldsymbol{\theta}_i) \\ \mathbf{Q}_i &\equiv \int d\mathbf{e}_i^s d\mathbf{x}_i d\boldsymbol{\theta}_i \left[\nabla_{\mathbf{g}} \mathcal{L}(\mathbf{D}_i | \mathbf{e}_i^s \oplus \mathbf{g}, \boldsymbol{\theta}_i) \Big|_{\mathbf{g}=0} \right] P_0(\mathbf{e}_i^s, \boldsymbol{\theta}_i) \\ \mathbf{R}_i &\equiv \int d\mathbf{e}_i^s d\mathbf{x}_i d\boldsymbol{\theta}_i \left[\nabla_{\mathbf{g}} \nabla_{\mathbf{g}} \mathcal{L}(\mathbf{D}_i | \mathbf{e}_i^s \oplus \mathbf{g}, \boldsymbol{\theta}_i) \Big|_{\mathbf{g}=0} \right] P_0(\mathbf{e}_i^s, \boldsymbol{\theta}_i) \end{aligned} \quad (23)$$

We would expect Equations (20) to be the more computationally efficient approach, since the derivatives of the prior with respect to shear can be pre-calculated once, whereas (23) require calculating 5 shear derivatives of the likelihood for every target galaxy. Furthermore the isotropy and parity symmetries of the unlensed sky simplify the shear derivatives of the prior.

3.2. Simplified demonstration

3.2.1. Adopted model

A numerical test with a simplified model demonstrates the accuracy and feasibility of the Bayesian shear estimates in the presence of highly non-Gaussian likelihoods for the ellipticities of

individual galaxies. We take a minimal set of galaxy properties to be $\mathbf{G} = \mathbf{e}^o$, the two components of a (post-lensing) true galaxy shape. We take an absolute minimal data vector $\mathbf{D}_i = \mathbf{e}^m$ for each galaxy to be a measurement of the ellipticity, ignoring centroid and any structural parameters. For each galaxy we:

- Draw a source ellipticity e^s from an isotropic unlensed distribution truncated to $e^s = |e^s| < 1$ and defined by

$$P_0(e^s) \propto [1 - (e^s)^2]^2 \exp[-(e^s)^2/2\sigma_{\text{prior}}^2]. \quad (24)$$

The additional factor of $(1 - (e^s)^2)^2$ atop the Gaussian ensures the prior has two continuous derivatives at the $|e| < 1$ boundary.

- Generate a lensed ellipticity $\mathbf{e}^o = \mathbf{e}^s \oplus \mathbf{g}$ for a constant shear \mathbf{g} , using the full non-Euclidean transformation for ellipticity under shear *e.g.* as described by Seitz & Schneider (1997).
- Obtain a measurement \mathbf{e}^m by drawing from a Gaussian distribution with a variance of σ_m^2 per axis. This measurement error is made non-Gaussian by truncation to $|e^m| < 1$. Furthermore we model biases in the measurement process by centering the Gaussian at a value $\mathbf{e}_{\text{ctr}} = (1 + m_{\text{bias}})\mathbf{e}^o + \mathbf{e}_{\text{bias}}$ for some multiplicative error m_{bias} and additive error \mathbf{e}_{bias} . In the numerical tests below, we adopt $m_{\text{bias}} = -0.1$ and $\mathbf{e}_{\text{bias}} = (0.03, 0)$.

The likelihood $\mathcal{L}(\mathbf{D}_i|\mathbf{G}) = \mathcal{L}(\mathbf{e}_i^m|\mathbf{e}^o)$ is a known truncated, biased function. The measurement error distribution is asymmetric with non-zero mean, and strongly dependent upon the intrinsic ellipticity—characteristics which induce biases in most extant shear-estimation methods.

3.2.2. Integration algorithm

The integrals in (20) are evaluated using a grid-based approach adapted from Miller et al. (2013). We define a set of sampled points, starting by evaluating the integrand of P_i in (20) at a random point in \mathbf{e}^o . We construct a square grid with initial resolution Δe centered on the initial sample. We then iterate this process:

1. Evaluate the integrand at all grid points that neighbor existing members of the sample.
2. Determine the maximum integrand value I_{max} among all sampled points.
3. Discard any sampled point with integrand $< t_{\text{min}}I_{\text{max}}$.

We iterate this process until no new samples are added on an iteration.

If the number of surviving above-threshold samples is $\geq N_{\text{min}}$, we halt the process. Otherwise we decrease the grid spacing Δe by a factor of $\sqrt{2}$ by adding a new grid point at the center of each

previous grid square. We then repeat the above iteration. The grid is refined until we reach the desired number of above-threshold samples or until we reach a minimum resolution. We can now calculate the integrals in (20) for each galaxy by summing over the sampled points e_{ij} :

$$P_i = \sum_j (\Delta e)^2 P(\mathbf{e}_i^m | \mathbf{e}_{ij}^o) P_0(\mathbf{e}_{ij}^o). \quad (25)$$

and evaluate \mathbf{Q}_i and \mathbf{R}_i by summing over the same samples, reusing the calculated $\mathcal{L}(\mathbf{e}^m | \mathbf{e}^o)$, changing only the last terms as per the integrands in (20).

3.2.3. Results

For all tests we fix $\sigma_{\text{prior}} = 0.3$, $\mathbf{g} = (0.01, 0)$, and $N_{\text{min}} = 50$. For each parameter set we simulate at least 0.75×10^9 galaxies to reduce the shape noise below our desired accuracy.

The left plot in Fig. 1 shows the relative error $|\bar{\mathbf{g}} - \mathbf{g}|/|\mathbf{g}|$ for different values of t_{min} and σ_m . The shaded region is the desired relative shear error of $|m| < 1 \times 10^{-3}$. We recover \mathbf{g} to this desired precision for all values of σ_m as long as t_{min} is below 10^{-4} , even when the shear measurement error is as large as $\sigma_m = 0.5$, as one might obtain for real galaxies with $S/N \approx 4$. The number of likelihood evaluations per galaxy is between 50 and 200 for all cases tested.

We also use a jackknife method to measure the statistical uncertainty in the shear estimator (7) from each simulation. The measured uncertainty in the shear is found to agree (to 1–2%) with the covariance matrix \mathbf{C}_g derived in (6) from the Bayesian framework.

The toy model illustrates the validity of the weak-shear Bayesian formalism in the face of non-Euclidean shear transformations and messy (but known) shape measurement errors.

The right-hand plot in Figure 1 plots the Bayesian shear measurement error vs the per-galaxy ellipticity measurement error σ_m , for the case $t_{\text{min}} = 10^{-7}$. For comparison we plot in blue the shear estimated for the same simulated data using the LENSFIT estimator described in section 2.5 of Miller et al. (2007). A galaxy weighting function is allowed in LENSFIT: we assume equal weighting for our simulated galaxies. The fully Bayesian shear estimator attains the desired $\Delta g/g < 0.1\%$ while the LENSFIT estimator does not. Note that Miller et al. (2013) present a different LENSFIT estimator which has been applied to the Canada-France-Hawaii Lens Survey.

3.3. Errors from unrecognized structural parameters

The primary difficulty of implementation of these Bayesian shear measurement methods will be the need to construct high-dimensional priors. We will be tempted to reduce the dimensionality of the galaxy parameter space. Under what circumstances can we omit a parameter from our Bayesian calculation and still obtain a rigorously correct result? Consider the simple case where a

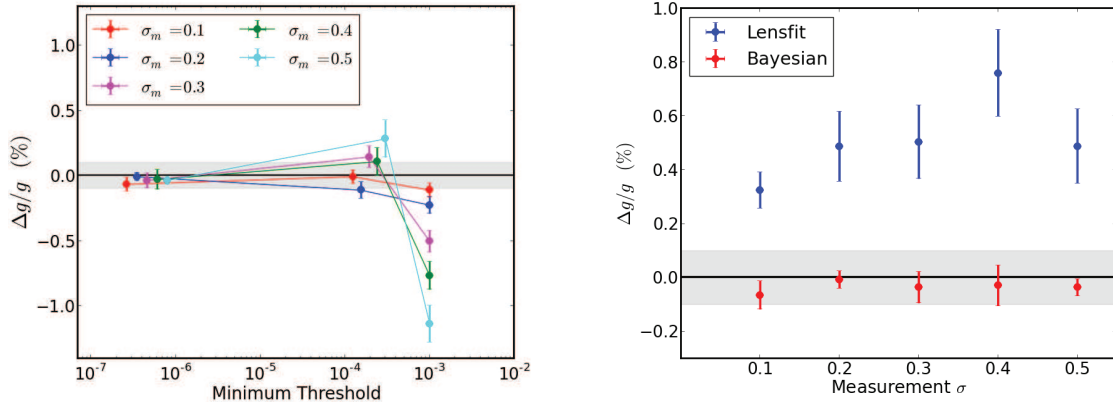


Fig. 1.— At left, the accuracy to which we are able to recover the reduced shear \mathbf{g} in our toy model is shown as a function of probability threshold t_{\min} (below the maximum) above which we keep points for the integration. The different curves show the accuracy for different ellipticity measurement errors σ_m . The shaded region shows the desired level of accuracy $m = \Delta g/g < 10^{-3}$ on \mathbf{g} . For $t_{\min} < 10^{-4}$ we find shear estimation with the desired accuracy. At right are the results for $t_{\min} = 10^{-7}$ showing the desired accuracy is obtained even for quite large, biased, non-Gaussian measurement errors in the model. Estimation of shear for the simulated data from the LENSFIT formulae of Miller et al. (2007) yields biases up to $\approx 10\times$ larger than our targets.

galaxy property set \mathbf{G} is supplemented by a parameter α which can take discrete values $\alpha_1, \alpha_2, \dots$ with probability p_1, p_2, \dots . The posterior contribution from a single galaxy is

$$P(\mathbf{D}_i|\mathbf{g}) \propto \int d\mathbf{G} \sum_j \mathcal{L}(\mathbf{D}_i|\mathbf{G}, \alpha_j) P(\mathbf{G}|\mathbf{g}, \alpha_j) p_j. \quad (26)$$

If we are unaware of this parameter or choose to ignore it, we will have a prior marginalized over α and probably assign a likelihood that is also an average over the α cases. Our posterior calculation will then yield

$$P(\mathbf{D}_i|\mathbf{g}) \propto \int d\mathbf{G} \left(\sum_j p_j \mathcal{L}(\mathbf{G}, \alpha_j) \right) \left(\sum_j p_j P(\mathbf{G}|\mathbf{g}, \alpha_j) \right). \quad (27)$$

This can differ from the correct (26) unless either the prior or data likelihood is independent of α . In other words: *the prior must specify the distribution of all galaxy parameters that the likelihood depends upon.*

We illustrate such bias by dividing the galaxies in our toy model into two populations A and B with distinct σ_{prior} and σ_m . Galaxies are assigned to Type B at random with some probability α_B . An observer ignorant of the existence of Type A and Type B galaxies would infer a prior and a measurement-error distribution that are found by averaging over the full population as in (27). Fig. 2 shows the accuracy of the Bayesian shear estimate under these (mistaken) assumptions. We

choose $\sigma_{\text{prior}A} = 0.1$, $\sigma_{\text{prior}B} = 0.3$, $\sigma_{mA} = 0.2$, and vary σ_{mB} . As expected a shear bias (up to 15%) appears as σ_{mB} becomes more distinct from σ_{mA} . The shear bias decreases when Type B galaxies become rarer and when their measurement error (hence likelihood function) become indistinguishable from Type A.

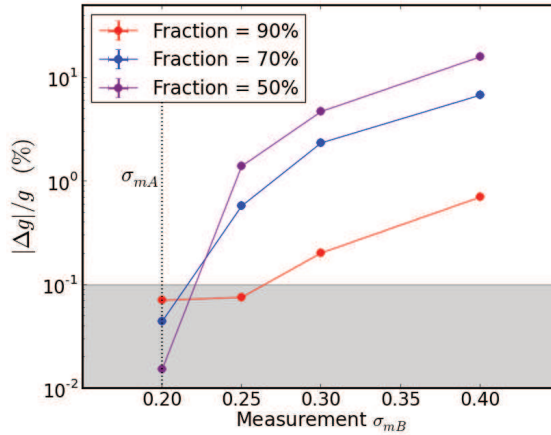


Fig. 2.— The multiplicative shear bias induced by the unrecognized presence of two galaxy populations A and B is plotted vs the measurement error σ_{mB} of the B population. The A population has measurement error $\sigma_{mA} = 0.2$. The intrinsic ellipticity dispersions for A and B galaxies are 0.1 and 0.3, respectively. The shear bias from the unrecognized structural parameter vanishes when the error distributions match and $\mathcal{L}(\mathbf{D}|\mathbf{e}^o)$ becomes independent of galaxy type. It is also reduced as the fraction α_B of the population in Type B is decreased.

For this Bayesian model-fitting method, an example of a galaxy parameter that can be ignored is color, which does not affect the likelihood function of single-band pixel data as long as the other parameters $\{\mathbf{e}, \mathbf{x}, \boldsymbol{\theta}\}$ completely specify the single-band appearance of the galaxy. The accuracy of the Bayesian inference may be improved, however, if we can include measured color in the data vector and include color dependence in the prior, *e.g.* by distinguishing late- and early-type galaxies.

In model-fitting, ignoring parameters that *do* affect the likelihood of pixel values can produce bias. An example would be assuming a fixed bulge-to-disk ratio when fitting a population of galaxies that has varying ratios.

Unfortunately there is no known finite parameterization for real galaxies’ appearances, and hence it is not possible to create a formally correct Bayesian model-fitting shear method for real galaxies. The means by which incomplete galaxy models can bias shear measurements are illustrated and explained by Voigt & Bridle (2010), Melchior & Viola (2012), and Bernstein (2010).

The potential for shear biases from unrecognized galaxy characteristics is not limited to model-fitting methods. For example in the model-free moment-based method described in the next section,

the Bayesian formalism will break down if the likelihood of the moments depends on the detailed structure of the underlying galaxy. As noted above, we need to marginalize over any galaxy parameter that appears in the likelihood expression for the data.

4. $P(\mathbf{D}_i|\mathbf{g})$ via data compression

4.1. General Formulation

Acknowledging that we cannot construct a model of galaxy structure with which to predict all pixel values, we can instead compress the pixel data into a small number of quantities that carry most of the information on any shear applied to the source. We will call the compressed quantities “moments” since we propose that they be intensity-weighted moments. This method will hence resemble the venerable Kaiser et al. (1995) shear-measurement methodology, but with critical changes to eliminate the approximations inherent to KSB and a rigorous Bayesian formulation to eliminate noise-induced biases.

We choose to reduce the pixel data for any galaxy image to a small vector $\mathbf{M} = \{M_1, M_2, \dots, M_m\}$ of derived quantities which we will select to be sensitive to shear. The \mathbf{M} must be chosen such that one can propagate the pixel noise model to the moment vector. If \mathbf{M}_i are the moments calculated from the pixel data for galaxy i , we must be able to assign a likelihood $\mathcal{L}(\mathbf{D}_i|\mathbf{G}) = \mathcal{L}(\mathbf{M}_i|\mathbf{M})$ of producing the measured moments given that the galaxy has true (noiseless) moments \mathbf{M} . In this case the contribution to the shear posterior from galaxy i is

$$P(\mathbf{D}_i|\mathbf{g}) \propto \int d\mathbf{M} d\mathbf{x} \mathcal{L}(\mathbf{M}_i|\mathbf{M})P(\mathbf{M}|\mathbf{x}, \mathbf{g}) = \int d\mathbf{M} \mathcal{L}(\mathbf{M}_i|\mathbf{M}) \int d\mathbf{x} P(\mathbf{M}|\mathbf{x}, \mathbf{g}), \quad (28)$$

where $P(\mathbf{M}|\mathbf{x}, \mathbf{g})$ is the prior distribution of moments of a galaxy centered at \mathbf{x} given a local shear \mathbf{g} . The Taylor expansion of the prior can be written as

$$\int d\mathbf{x} P(\mathbf{M}|\mathbf{x}, \mathbf{g}) = P_0(\mathbf{M}) + \mathbf{g} \cdot \mathbf{Q}(\mathbf{M}) + \frac{1}{2}\mathbf{g} \cdot \mathbf{R}(\mathbf{M}) \cdot \mathbf{g} + O(g^3). \quad (29)$$

and then the quantities needed from each galaxy for the Bayesian posterior in Equation (5) are

$$\left\{ \begin{array}{c} P_i \\ \mathbf{Q}_i \\ \mathbf{R}_i \end{array} \right\} \equiv \int d\mathbf{M} \mathcal{L}(\mathbf{M}_i|\mathbf{M}) \left\{ \begin{array}{c} P_0(\mathbf{M}) \\ \mathbf{Q}(\mathbf{M}) \\ \mathbf{R}(\mathbf{M}) \end{array} \right\} \quad (30)$$

Now the operative procedure for obtaining the Bayesian shear is:

1. Determine the prior $P(\mathbf{M}|\mathbf{x}, \mathbf{g})$ from a high- S/N imaging sample, and perform the Taylor expansion in Equation (29). Here \mathbf{x} is the vector from the coordinate origin of the moments to the center of the galaxy. The derivatives of this prior under shear must be obtained by

simulating the action of shear on each member of the high- S/N ensemble defining the prior. Appendix B shows that the derivatives of the moments \mathbf{M} are equal to a set of higher-order moments, which can hence be measured directly from the high- S/N sample. There is no longer any explicit ellipticity parameter describing each galaxy to represent the shear-dependent aspects of that galaxy.

2. For each observed galaxy, measure the moments \mathbf{M}_i of that galaxy about some pre-selected coordinate origin and determine the likelihood function $\mathcal{L}(\mathbf{M}_i|\mathbf{M})$. We have no further need of the pixel data for the galaxy after this compression.
3. Compute the six distinct integrals in (30) over the moment space \mathbf{M} to get P_i, \mathbf{Q}_i , and \mathbf{R}_i . This is the computationally intensive step.
4. Sum over galaxies to obtain \mathbf{C}_g^{-1} in Equation (6).
5. Sum over galaxies to obtain the shear estimate $\bar{\mathbf{g}}$ as in Equation (7). The shear posterior has this mean (and maximum) and covariance matrix \mathbf{C}_g .

4.2. A specific choice of data compression

To make things more concrete, we propose that the compressed quantities \mathbf{M} be intensity-weighted moments of the galaxy image. We will evaluate these in Fourier domain where, in the absence of aliasing, the exact correction for the effect of the point spread function (PSF) on the observed galaxy image is a simple division. This yields our Bayesian Fourier-domain (BFD) algorithm. The moment vector could be

$$\begin{pmatrix} M_I \\ M_x \\ M_y \\ M_r \\ M_+ \\ M_\times \end{pmatrix} = \int d^2k \frac{\tilde{I}^o(\mathbf{k})}{\tilde{T}(\mathbf{k})} W(|\mathbf{k}^2|) \begin{pmatrix} 1 \\ ik_x \\ ik_y \\ k_x^2 + k_y^2 \\ k_x^2 - k_y^2 \\ 2k_x k_y \end{pmatrix}. \quad (31)$$

Here $\tilde{I}^o(\mathbf{k})$ and $\tilde{T}(\mathbf{k})$ are the Fourier transforms of the observed image and the PSF, respectively, and $W(|\mathbf{k}^2|)$ is a window function applied to the integral to bound the noise, in particular confining the integral to the finite region of k in which $\tilde{T}(\mathbf{k})$ is non-zero, as detailed in Bernstein (2010). There is a specific weight that will offer optimal S/N for a given galaxy+PSF pair, but any properly bounded weight with finite 2nd derivatives produces a valid shear method. One can select a single weight function for a full survey and retain good S/N as long as the PSF does not vary widely in size. In real data the integrals revert to sums over the k -space values sampled by a discrete Fourier transform (DFT) of the pixel data D_i .

The first motivation for this choice is that these moments are linear in the observed pixel data and therefore meet the requirement that we be able to construct a moment noise model $\mathcal{L}(\mathbf{M}_i|\mathbf{M})$ from the known pixel noise model. In fact if the noise in the pixels is independent of the pixel values, then the covariance matrix \mathbf{C}_i of the moments is independent of the value of \mathbf{M} , and also independent of any other properties of the galaxy. Such is the case for the background-limited conditions typical of faint-galaxy imaging. If the noise is stationary, than all galaxies with the same PSF will have the same \mathbf{C}_i . Even if the pixel noise is not Gaussian, the central limit theorem implies that the moments, which are sums over many independent pixels, will tend toward a Gaussian distribution. We therefore can take

$$-2 \ln \mathcal{L}(\mathbf{M}_i|\mathbf{M}) = \ln |2\pi\mathbf{C}_i| + (\mathbf{M}_i - \mathbf{M}) \cdot \mathbf{C}_i^{-1} \cdot (\mathbf{M}_i - \mathbf{M}). \quad (32)$$

Furthermore if the PSF is (nearly) isotropic, then the azimuthal symmetries of our chosen basis set guarantee that \mathbf{C}_i will be (nearly) diagonal, with the exception of a covariance between the two monopole moments M_I and M_r .

One departure from common shear-measurement practices is that calculating \mathbf{M}_i from pixel data for i does not involve any iterative procedures such as centroiding, since iteration usually produce non-analytic likelihoods. In Section 5 we look for feasible approximations to the propagation of errors into some iterative compressed quantities.

We are also tempted to reduce the dimensionality of our prior and speed up marginalization by working with the normalized ratios M_x/M_I , M_y/M_I , M_+/M_r , and M_\times/M_r that figure prominently in KSB, then dropping M_I and M_r from our data vector. The probability distribution for such ratios of Gaussian deviates is known (Melchior & Viola 2012), but depends on the mean value and variance of the denominator, so the moment likelihood function would still depend on M_I and M_r . As per the discussion in Section 3.3, we would still need to include these quantities in the prior and marginalize over them, foiling our plan to simplify the prior. We choose the straightforward path of compressing the pixel data to un-normalized moments.

What is the motivation for choosing this particular set of linear moments? Any choice of well-defined compressed data vector \mathbf{M} will yield a *valid* Bayesian shear estimator under this method, but the choices will differ in the *precision* to which they determine the shear \mathbf{g} from a given galaxy sample. We want \mathbf{M} to include quantities that unambiguously capture most of the impact of shear upon the pixel image. The quadrupole moments M_+ and M_\times respond at first order to shear. They are also sensitive at first order to the galaxy size and flux, and at second order to translation of the galaxy image, so we add the monopole and dipole moments M_I , M_r , M_x , and M_y , sensitive to flux, size, and translation in first order, to yield less degenerate shear information for each galaxy. The inclusion of M_r furthermore would admit generalizing the Bayesian formalism to infer the weak lensing magnification μ along with the 2 shear components \mathbf{g} .

4.3. Generating the Prior

We defer testing of a full implementation of this method for a later publication, but we do outline the necessary steps and possible economies.

The biggest astrophysical challenge will be to produce the prior, which is a function of the six \mathbf{M} components—which can be reduced to 5 dimensions because the isotropy of the Universe requires the unlensed prior to be invariant under coordinate rotation. At each point in the 5-dimensional space, we require 5 shear derivatives of the prior as well as the unsheared prior, so the we must construct a 6-dimensional function on a 5-dimensional space, and for each source galaxy integrate the posterior over all 6 dimensions of \mathbf{M} . Note that this BFD method will be much faster than the BMF method even at equal dimensionality, because BFD requires the evaluation of only one Gaussian $\mathcal{L}(\mathbf{M}_i|\mathbf{M})$ at each point of the integration, whereas BMF requires evaluation of the full likelihood of the pixel data of a model.

Since galaxy-evolution theory will not be able in the foreseeable future to provide an *a priori* distribution of galaxy appearances, the prior will always have to be empirical. The prior can be established by obtaining high- S/N data on a sample of the sky. Note that the \mathbf{M} values depend upon the choice of weight function W to suit the observational PSF, and implicitly depend upon the filter passband used for the observations, so the prior is best constructed from deep integrations using the same instrument as the main survey. The number of high- S/N galaxies necessary to adequately define the prior is an important issue for future study.

The prior can be generated by some kernel density estimation over the empirical moments \mathbf{M}_μ where μ indexes the members of the high- S/N template galaxy set. In (28), however, we see that the prior is already being convolved with the likelihood function for a target galaxy. Hence if the we are using target galaxies of sufficiently low S/N that $\mathcal{L}(\mathbf{M}_i|\mathbf{M})$ is broad enough to sample many elements of the template set, it is adequate to express the prior as a sum of delta functions for each template galaxy:

$$P(\mathbf{M}|\mathbf{g}) \propto \sum_{\mu} \delta^m [\mathbf{M} - \mathbf{M}_\mu(\mathbf{g})], \quad (33)$$

where we need $\mathbf{M}_\mu(\mathbf{g})$, the moments for the template galaxy if it were sheared by \mathbf{g} . The posterior contribution for galaxy i becomes

$$P(\mathbf{D}_i|\mathbf{g}) \propto \sum_{\mu} \mathcal{L}[\mathbf{M}_i|\mathbf{M}_\mu(\mathbf{g})]. \quad (34)$$

We perform a Taylor expansion on this shear-conditioned probability to obtain our required prop-

erties:

$$\begin{aligned}
 P_i &= \sum_{\mu} \mathcal{L}(M_i | M_{\mu}), \\
 Q_i &= \sum_{\mu} \left[\frac{\partial}{\partial M} \mathcal{L}(M_i | M) \right]_{M_{\mu}} \cdot \nabla_{\mathbf{g}} M_{\mu}, \\
 R_i &= \sum_{\mu} \nabla_{\mathbf{g}} M_{\mu} \cdot \left[\frac{\partial^2}{\partial M^2} \mathcal{L}(M_i | M) \right]_{M_{\mu}} \cdot \nabla_{\mathbf{g}} M_{\mu} \\
 &\quad + \sum_{\mu} \left[\frac{\partial}{\partial M} \mathcal{L}(M_i | M) \right]_{M_{\mu}} \cdot \nabla_{\mathbf{g}} \nabla_{\mathbf{g}} M_{\mu},
 \end{aligned} \tag{35}$$

where all moments and derivatives are taken at $\mathbf{g} = 0$. The determination of $\nabla_{\mathbf{g}} M_{\mu}$ from the data for template galaxy μ is straightforward in Fourier domain, and is given in Appendix B.

Now we adopt the multivariate Gaussian likelihood (32) for the moments. We also can define $\mathbf{M}_{\mu}(\mathbf{x}, \phi)$ to be the moments that we would assign to template galaxy μ if it were translated to \mathbf{x} (relative to the target galaxy’s coordinate origin) and rotated by ϕ . Because the unlensed sky is isotropic, we can assume that the true prior contains replicas of template galaxy μ at all \mathbf{x} and ϕ .³ The parity invariance of the unlensed sky also implies that we can place a mirror image of each template galaxy in the prior as well. Appendix B shows how to calculate moments for these transformed versions of a template galaxy.

For notational simplicity we will subsume the parity flip into the integration over rotation ϕ . The Taylor-expanded posterior derived from the template sample now becomes:

$$\begin{aligned}
 P_i &= \sum_{\mu} \int d\mathbf{x} d\phi \mathcal{L}_{i\mu}(\mathbf{x}, \phi) \\
 Q_i &= \sum_{\mu} \int d\mathbf{x} d\phi \mathcal{L}_{i\mu}(\mathbf{x}, \phi) [\mathbf{M}_i - \mathbf{M}_{\mu}(\mathbf{x}, \phi)] \cdot \mathbf{C}_i^{-1} \cdot \nabla_{\mathbf{g}} M_{\mu}(\mathbf{x}, \phi) \\
 R_i &= \sum_{\mu} \int d\mathbf{x} d\phi \mathcal{L}_{i\mu}(\mathbf{x}, \phi) \{ [\mathbf{M}_i - \mathbf{M}_{\mu}(\mathbf{x}, \phi)] \cdot \mathbf{C}_i^{-1} \cdot \nabla_{\mathbf{g}} \nabla_{\mathbf{g}} M_{\mu}(\mathbf{x}, \phi) \\
 &\quad + \nabla_{\mathbf{g}} M_{\mu}(\mathbf{x}, \phi) \cdot \mathbf{C}_i^{-1} \cdot \nabla_{\mathbf{g}} M_{\mu}(\mathbf{x}, \phi) \} \\
 \mathcal{L}_{i\mu}(\mathbf{x}, \phi) &\equiv \exp \left\{ -\frac{1}{2} [\mathbf{M}_i - \mathbf{M}_{\mu}(\mathbf{x}, \phi)] \cdot \mathbf{C}_i^{-1} \cdot [\mathbf{M}_i - \mathbf{M}_{\mu}(\mathbf{x}, \phi)] \right\}
 \end{aligned} \tag{36}$$

The computational challenge of this Bayesian Fourier-domain shear inference is the high multiplicity of this calculation: for every target galaxy i , we collect 6 sums over every template galaxy

³We can limit the potential positions \mathbf{x} of the template galaxy centroid to be within the range of pixels assigned to our target galaxy i , essentially adopting a prior that we have indeed found a galaxy and its center is within our postage stamp. This avoids the problem of divergent position marginalization noted in Miller et al. (2013).

μ , with each term of each sum being an integral of a Gaussian function of the three dimensions plus parity flip of (\mathbf{x}, ϕ) . There are obvious efficiencies to be gained in this calculation by pruning the template set to those with significant contributions to the sums. Furthermore we recall that all science will come from sums over a large number of target galaxies, so we can subsample the template set when computing the posterior for individual target galaxies, if we can do so without inducing systematic biases on $(P_i, \mathbf{Q}_i, \mathbf{R}_i)$.

A substantial speedup of the Bayesian shear calculation is enabled if we can approximate \mathbf{M}_μ as linearly dependent on \mathbf{x} , in which case two of the three dimensions of the integrals in Equations (36) reduce to linear algebra. Appendix B shows how to determine these derivatives for the template galaxies.

We leave the testing of a practical implementation of Equations (36) and the investigation of the required size of the template galaxy sample to further work.

5. $P(D_i|g)$ via null tests

The BFD method improves on the BMF method by eliminating the approximation that target galaxies are described by a low-dimensional model. We paid a price, however, in losing the convenience of having the action of shear be fully described by alteration of just the two components of \mathbf{e} . This allowed us to derive the lensed prior solely from derivatives with respect to e of the unlensed prior $P_0(e, \boldsymbol{\theta})$. In this Section we ask whether null-testing methods can be used to make a model-free Bayesian shear inference with the simplicity of a known shear transformation $\mathbf{e} \oplus \mathbf{g}$. We conclude below that this is difficult. Readers uninterested in the null-testing approach can safely skip this section.

Windowed centroiding procedures assign a center \mathbf{x} to a galaxy by translating the galaxy until the windowed first moments are nulled. The galaxy is assigned a centroid that is the inverse of the translation needed to null the moments. In the Fourier Domain Null Test (FDNT) method (Bernstein 2010), this is extended by shearing as well as translating the galaxy (after correcting for seeing) until we null the moments M_x, M_y, M_+ , and M_\times in Equation (31). The galaxy is assigned a shape \mathbf{e}_i that is the inverse of the shear that produces the null. The moment vector for galaxy i is hence a function $\mathbf{M}_i(\mathbf{E})$ of the four-dimensional transformation $\mathbf{E} = (\mathbf{g}, \mathbf{x})$ and we assign the galaxy a shape and centroid $\mathbf{E}_i = (\mathbf{e}_i, \mathbf{x}_i)$ such that $\mathbf{M}_i(-\mathbf{E}_i) = 0$. This approach assures a well-determined transformation of the measured shape \mathbf{e}_i under an applied shear \mathbf{g} , and there is no need of a galaxy model. Bernstein (2010) demonstrates shear inferences errors of < 1 part in 10^3 on low-noise data using FDNT.

The application of rigorous Bayesian formalism to FDNT is foiled, however, because there is no straightforward means of propagating the pixel noise model to a likelihood $\mathcal{L}(\mathbf{E}_i|\mathbf{E})$ of measuring a null at \mathbf{E}_i when the underlying galaxy has true null at \mathbf{E} . It is possible, however, to approximate $\mathcal{L}(\mathbf{E}_i|\mathbf{E})$ in the case where the measured shape and centroid are close to the true ones. At sufficiently

high S/N of the target galaxy, the likelihood will be confined to such regions and the Bayesian formulation with this approximation will become accurate.

The measured moments \mathbf{M}_i for galaxy i when transformed by \mathbf{E} can be written as

$$\mathbf{M}_i(\mathbf{E}) = \mathbf{M}_\mu(\mathbf{E}) + \delta\mathbf{M}_i(\mathbf{E}), \quad (37)$$

where \mathbf{M}_μ is the true underlying moment and $\delta\mathbf{M}_i$ is the variation induced by measurement noise. Since $\mathbf{M}_i(\mathbf{E})$ is a linear function of the pixel data, the likelihood $\mathcal{L}_i[\delta\mathbf{M}_i(\mathbf{E})]$ is calculable and close to Gaussian.

Our first approximation is to linearize \mathbf{M}_μ about the \mathbf{E}_μ that nulls it:

$$\mathbf{M}_\mu(\mathbf{E}) = \mathbf{D}_\mu \cdot (\mathbf{E} - \mathbf{E}_\mu), \quad (38)$$

$$\mathbf{D}_\mu \equiv \left. \frac{\partial \mathbf{M}_\mu}{\partial \mathbf{E}} \right|_{\mathbf{E}_\mu}. \quad (39)$$

Second we assume that $\delta\mathbf{M}_i(\mathbf{E})$ is invariant in the neighborhood of \mathbf{E}_i and that this measurement error has a multivariate Gaussian likelihood $\mathcal{L}_i(\delta\mathbf{M})$ defined by a covariance matrix \mathbf{C}_i and zero mean. Then via Equation (37) the nulling transformation \mathbf{E}_i is

$$0 = \mathbf{M}_i(\mathbf{E}_i) = \mathbf{D}_\mu \cdot \delta\mathbf{E}_{i\mu} + \delta\mathbf{M}_i \quad (40)$$

$$\Rightarrow \mathcal{L}(\mathbf{E}_i|\mathbf{E}_\mu) = \mathcal{L}_i(-\mathbf{D}_\mu \cdot \delta\mathbf{E}_{i\mu}) |\mathbf{D}_\mu|. \quad (41)$$

If we again construct the prior from a template set of galaxies indexed by μ , having ellipticities \mathbf{e}_μ , and uniformly distributed in position \mathbf{x}_μ with respect to the target galaxy's position, then the contribution to the posterior from target galaxy i is the sum over template galaxies:

$$P(\mathbf{E}_i|\mathbf{g}) \propto \sum_\mu \int d^2x_\mu |\mathbf{D}_\mu| \exp \left[-\frac{1}{2} \delta\mathbf{E}_{i\mu}^T \mathbf{D}_\mu^T \mathbf{C}_i^{-1} \mathbf{D}_\mu \delta\mathbf{E}_{i\mu} \right]. \quad (42)$$

The integration over the two spatial dimensions \mathbf{x}_μ of the Gaussian argument $\mathbf{E}_\mu = (\mathbf{e}_\mu, \mathbf{x}_\mu)$ is analytic. To complete the implementation of the Bayesian framework we need to find the Taylor expansion of Equation (42) with respect to \mathbf{g} . The right-hand side depends implicitly on the applied shear \mathbf{g} because the template galaxy's shape \mathbf{e}_μ is transformed by applied shear and enters into $\delta\mathbf{E}_{i\mu}$. To be thorough we should also account for the variation of the derivative vector \mathbf{D}_μ with applied shear. Doing so is straightforward but not instructive so we omit the algebra here.

We find therefore that there is a high- S/N approximation to the Bayesian shear estimator in the case of iterative null tests, but that this requires knowing the prior distribution not only of the galaxies' ellipticities \mathbf{e} but also of the derivatives \mathbf{D} of the null tests with respect to shear and translation. Hence even in the high- S/N approximation, we have not found a way to produce a simpler model-free derivatives of the prior than in BFD. We will therefore choose to pursue BFD first, as it demands no approximations beyond the weak-shear Taylor expansion of the posterior and does not require searching for nulled moments.

6. Comparison to other methods

6.1. Model fitting

The BMF shear measurement that we propose bears very close resemblance to LENSFIT. LENSFIT is described as “Bayesian galaxy shape measurement” and differs from our BMF method which is derived as a Bayesian *shear* determination. The consequence is that BMF does not assign shapes (ellipticities) to galaxies, instead computing the likelihood-weighted derivatives of the prior for each galaxy as per (20), and combining to yield shear as per (6) and (7).

LENSFIT already does the hard computational work of our BMF algorithm, namely the integration of the data likelihood times the prior over the parameters of the model space. Hence LENSFIT serves as an example of the feasibility of our BMF method. At a minimum level of realism, the galaxy model must include two ellipticity components \mathbf{e} , two centroid components \mathbf{x} , and $\boldsymbol{\theta}$ including a galaxy flux, size, and a measure of concentration such as the Sersic index, for 7 parameters. Isotropy reduces the unlensed prior to 6 dimensions. The posterior requires integration over 7 dimensions. Miller et al. (2007) reduce the dimensionality of the likelihood integral by analytic marginalization over flux (which requires a particular choice of prior) and linearization of the model dependence on \mathbf{x} . Miller et al. (2013) use a bulge/disk ratio in place of a Sersic index for concentration. Their work hence demonstrates the feasibility of computing the Bayesian integrals over a 7-dimensional model space. The LENSFIT implementations simplify the prior substantially by separating the dependence on variables. A numerical approach to constructing an accurate fully-coupled prior from high- S/N observations remains to be demonstrated.

There are reasons to suspect that this minimal model does not describe the true galaxy population sufficiently well to achieve $|m| < 10^{-3}$, in particular because galaxies with radial gradients in ellipticity induce biases in shear inferences when fit by models without gradients (Bernstein 2010). The computational difficulty will grow, with an exponential increase in the number of likelihood evaluations, as additional parameters are needed in the model and hence in the prior and the integrations. This will lead us to favor the BFD method. Model-fitting will remain useful, however, in cases of incomplete pixel information on the galaxy, *e.g.* from cosmic rays, in which case the models can serve as a sparse dictionary for the pixel data.

6.2. Moment compression

The Bayesian Fourier Domain (BFD) method is model-free, in common with many moment-based schemes for shear inference, the best-known of which is from Kaiser et al. (1995, KSB). BFD shares with KSB and its brethren the approach that the galaxy pixel data can be compressed to a few simple moments which transmit most of the information on lensing shear of the image. The BFD method, however, differs fundamentally in explicit use of a prior high- S/N moment distribution, as opposed purely to summations over properties of the normal- S/N images. There

are fundamental differences between BFD and KSB that give the former a rigorous treatment of the effects of PSFs and noise:

- The BFD method accumulates moments in Fourier domain, admitting an exact correction for the joint effects of the PSF and shear on the images, avoiding the need for KSB’s Gaussian-based approximations.
- The BFD method does not require an iterative centroiding procedure, meaning the full likelihood of the observed moments remains known even at low S/N . Positional uncertainties are treated by Bayesian integration over all possible positions of the galaxy.
- The “polarizability” that KSB calculates for each galaxy is effectively replaced by integration of the target galaxy’s moment likelihood over the shear derivatives of the prior. The BFD approach is exact in the presence of noise whereas the single-galaxy polarizabilities are biased by noise. A consequence of this is the absence of an ellipticity assignment to individual galaxies in BFD.

The non-Bayesian method bearing the closest resemblance to BFD is described by Zhang (2011) and its predecessor papers. Like BFD, Zhang’s method is equivalent to accumulating moments in Fourier domain, and emphasizes that a shear inferred from the ratio of two sums over the galaxy population—an average “signal” divided by an average “responsivity”—is less biased by noise than a shear inferred from a sum of single-galaxy ratios *a la* KSB. A critical difference is that Zhang’s method takes moments of the power spectrum $|\tilde{I}^2(\mathbf{k})|$ rather than the Fourier amplitude $\tilde{I}(\mathbf{k})$. This makes the method insensitive to the choice of centroid. It also, however, amplifies the noise relative to the signal and the rectified noise must be very precisely removed from the power spectrum. Neither Zhang nor KSB have an intrinsic means of appropriately weighting the galaxies for the shear information that they contain, which occurs naturally in the BFD method. This means they require some form of weighting or selection in order to keep the low- S/N galaxies from ruining the S/N of the shear inference. Weighting and selection can themselves induce biases in the inferred shear. Finally, Zhang’s method is formulated only for a Gaussian weight function $W(|k|)$, which formally requires integration over regions of k -space with infinite noise in any real image.

High shear fidelity on simulated images has been achieved by “stacking” methods, which sum galaxy images before analysis (Kuijken 1999; Lewis 2009). These work by essentially creating a single high- S/N image with an unlensed source that must approach circularity. Noise-induced biases are therefore avoided and the number of parameters needed to approximate the mean galaxy is greatly reduced. These stacking methods have practical drawbacks when the PSF and/or the lensing shear vary across the image. There is also a deeper problem in the need to assign an origin to each galaxy to build the stack. At this stage the galaxies’ individual low S/N levels are still present and noise-induced biases, primarily a suppression of the shear inferred from the stack, are important. The BFD method will avoid this problem.

7. Conclusion

We have shown how the exact Bayesian formulation of shear inference from a collection of galaxy images can be turned into a practical measurement technique in the limit of weak shear, by accumulating each target galaxy’s contribution to the first terms of the power-law expansion of the posterior $\ln P(\mathbf{g}|\mathbf{D})$. We can expect this rigorously derived treatment of noise to yield highly accurate shears even at low S/N , and also make it possible to suppress selection biases in the shear inference. We confirm the ability of the algorithm to provide part-per-thousand shear inference at low S/N , in the case of a highly simplified model of galaxy measurement.

The Bayesian derivation leads to a shear estimator that departs in significant ways from most previously proposed methods. Ellipticities (shapes) are not assigned to individual galaxies; biases are avoided by combining a large ensemble of low- S/N galaxies into a single shear estimator. Another important element is the marginalization over galaxy position rather than selecting a centroid. These elements have been used separately in previous methods, but not together.

There are two clear routes to coupling the Bayesian treatment of noise with an exact treatment of the effects of the PSF and sampling on the image: Bayesian Model Fitting (BMF) assumes the target galaxies follow known parameterized forms, and the pixel data can be compared to models that have the instrumental effects applied. BMF needs to know the distribution of the unlensed population over the model parameters. The LENSFIT code has demonstrated the computational feasibility of this approach for the minimal galaxy models. Any model-fitting approach is only accurate, however, insofar as the real galaxies hew to the models. Given the infinite variety of real galaxies, there is an inherent approximation remaining in the BMF method, which needs to be evaluated. Model-fitting methods do however have the advantage of working even with incomplete or aliased pixel data for a galaxy.

The second route, Bayesian Fourier Domain (BFD) inference, compresses both the target galaxies and the prior into a set of k -space moments. Exact corrections for PSF and sampling are possible and the method is model-free if the images are fully sampled. The likelihood of the (compressed) data given the underlying moment vector is a well-defined multivariate Gaussian in the common case of background-limited observations. We propose to apply the method to the zeroth, first, and second moments of the galaxies. Measuring these 6 moments will be fast and foolproof—no iteration is required. The prior distribution of moments will be 5-dimensional because of isotropy. We show how the prior can be constructed and integrated using empirical moment measurements on high- S/N images obtained from long integrations on a small subset of the sky area in a given survey. This integration is likely to be the most computationally intensive step of an implementation of the BFD method. The required size of this template subsample is an important issue for future study.

Both the BMF and BFD methods require empirical inputs in the form of distributions of real galaxies over some galaxy property vector \mathbf{G} —galaxy ellipticities, Sersic indices, etc. in the BMF case, and seeing-corrected galaxy moments in the BFD case. Also in either case one must know

how this empirical distribution changes under application of lensing shear (and magnification). In the BMF case, this typically is a simple shift of galaxy ellipticity parameters. In the BFD case, the derivatives of galaxy moments under shear are simply higher-order moments derived in Appendix B. Hence BFD is truly model-free in the sense that it is not necessary to characterize the full surface-brightness distributions of real galaxies—just the empirical distribution of a finite set of galaxy moments.

Both the BMF and BFD methods easily treat the cases of multiple exposures of a single galaxy, spatially varying shear and PSFs, and are extensible to the inference of lensing magnification as well as shear. While we defer testing of implementations of these methods to a future publication, the absence of approximations in the derivation of these methods, particularly the BFD method, gives great hope of achieving shear inference at better than part-per-thousand accuracy, as is required for future ambitious weak lensing surveys.

Both authors were supported by Department of Energy grant DE-SC0007901. GMB additionally acknowledges support from National Science Foundation grant AST-0908027 and NASA grant NNX11AI25G. We are grateful to Sarah Bridle, Bhuvnesh Jain, Mike Jarvis, Marisa March, and Lance Miller for conversations that have helped guide this work. We thank the referee, whose comments on this submission led us to significantly better presentation and understanding of the method described herein.

REFERENCES

- Bernstein, G. M. 2010, MNRAS, 406, 2793
- Bernstein, G., & Gruen, D. 2013, in preparation
- Bridle, S., Balan, S. T., Bethge, M., et al. 2010, MNRAS, 405, 2044
- Heymans, C., Van Waerbeke, L., Bacon, D., et al. 2006, MNRAS, 368, 1323
- Hoekstra, H., & Jain, B. 2008, Annual Review of Nuclear and Particle Science, 58, 99
- Huterer, D., Takada, M., Bernstein, G., & Jain, B. 2006, MNRAS, 366, 101
- Kacprzak, T., Zuntz, J., Rowe, B., et al. 2012, MNRAS, 427, 2711
- Kaiser, N., Squires, G., & Broadhurst, T. 1995, ApJ, 449, 460
- Kitching, T. D., Balan, S. T., Bridle, S., et al. 2012, MNRAS, 423, 3163
- Kuijken, K. 1999, A&A, 352, 355
- Lewis, A. 2009, MNRAS, 398, 471

- Massey, R., Heymans, C., Bergé, J., et al. 2007, MNRAS, 376, 13
- Melchior, P., & Viola, M. 2012, MNRAS, 424, 2757
- Miller, L., Kitching, T. D., Heymans, C., Heavens, A. F., & van Waerbeke, L. 2007, MNRAS, 382, 315
- Miller, L., Heymans, C., Kitching, T. D., et al. 2013, MNRAS, 429, 2858
- Refregier, A., Kacprzak, T., Amara, A., Bridle, S., & Rowe, B. 2012, MNRAS, 425, 1951
- Seitz, C., & Schneider, P. 1997, A&A, 318, 687
- Voigt, L. M., & Bridle, S. L. 2010, MNRAS, 404, 458
- Weinberg, D. H., Mortonson, M. J., Eisenstein, D. J., et al. 2013, Phys. Rep., 530, 87
- Zhang, J. 2011, J. Cosmology Astropart. Phys., 11, 41
- Zuntz, J., Kacprzak, T., Voigt, L., et al. 2013, MNRAS, 434, 1604

A. Third-order posterior calculation

Here we take the expansion for $\ln P(\mathbf{g}|\mathbf{D})$ to third order in g , and calculate the perturbation to the maximum and mean of the posterior relative to the second order (Gaussian) result in Section 2.1. We adopt a slightly different notation by first expanding the transformed prior as

$$P(\mathbf{e}^o|\mathbf{g}) = P_0(\mathbf{e}^o \oplus -\mathbf{g}) \left| \frac{d\mathbf{e}^s}{d\mathbf{e}^o} \right|_{-\mathbf{g}} \quad (\text{A1})$$

$$\begin{aligned} &= P_0(e) + q(e)g \cos \Delta\phi \\ &\quad + \frac{g^2}{2} [r_0(e) + r_2(e) \cos 2\Delta\phi] \\ &\quad + \frac{g^3}{6} [s_1(e) \cos \Delta\phi + s_3(e) \cos 3\Delta\phi]. \end{aligned} \quad (\text{A2})$$

Both the unlensed prior and the shear transformation formula must be invariant under rotation of coordinates, so the sheared prior must be a function only of the ellipticity amplitude $e = |\mathbf{e}^o|$, the shear amplitude $g = |\mathbf{g}|$, and the angle $\Delta\phi$ between them. Sine terms are absent because the shear transformation law should be invariant under parity flip.

The functions q, r_0, r_2, s_1 , and s_3 of galaxy ellipticity e can be expressed as algebraic combinations of derivatives of P_0 and of the shear addition law. These expressions are complex and not enlightening, and in practice a numerical estimate is likely to be faster than the algebraic calculation anyway, so we omit the algebraic forms. Throughout this Appendix we also omit the additional galaxy parameters $\boldsymbol{\theta}$ which will also be arguments of P_0 and the five derivative functions.

Adopting the complex notation $g = g_x + ig_y$, and designating ϕ as the azimuthal angle of \mathbf{e} , the posterior likelihood of shear for galaxy j becomes

$$P(\mathbf{g}|\mathbf{D}_i) \propto P_i + \text{Re} \left[Q_j^* g + \frac{1}{2} (R_{0j}^* g g^* + R_{2j}^* g^2) + \frac{1}{6} (S_{1j}^* g^2 g^* + S_{3j}^* g^3) \right], \quad (\text{A3})$$

$$\left\{ \begin{array}{c} P_j \\ Q_j \\ R_{0j} \\ R_{2j} \\ S_{1j} \\ S_{3j} \end{array} \right\} \equiv \int e \, de \, d\phi \, P(\mathbf{D}_j|\mathbf{e}) \left\{ \begin{array}{c} P_0(e) \\ q(e) \exp(i\phi) \\ r_0(e) \\ r_2(e) \exp(2i\phi) \\ s_1(e) \exp(i\phi) \\ s_3(e) \exp(3i\phi) \end{array} \right\}$$

After taking the logarithm of the posterior in (A3) to third order in g , we sum over galaxies

to get the (log of) the total shear posterior probability:

$$-\ln P(\mathbf{g}|\mathbf{D}) = -\sum \ln P_j + \text{Re} \left[Q^* g + \frac{1}{2} (R_0^* g g^* + R_2^* g^2) + \frac{1}{6} (S_1^* g^2 g^* + S_3^* g^3) \right], \quad (\text{A4})$$

$$-Q = \sum \frac{Q_j}{P_j}, \quad (\text{A5})$$

$$-R_0 = \sum \left(\frac{R_{0j}}{P_j} - \frac{1}{2} \frac{Q_j Q_j^*}{P_j^2} \right), \quad (\text{A6})$$

$$-R_2 = \sum \left(\frac{R_{2j}}{P_j} - \frac{1}{2} \frac{Q_j^2}{P_j^2} \right), \quad (\text{A7})$$

$$-S_1 = \sum \left(\frac{S_{1j}}{P_j} - 3 \frac{R_{0j} Q_j}{P_j^2} - \frac{3}{2} \frac{R_{2j} Q_j^*}{P_j^2} + \frac{3}{2} \frac{Q_j^2 Q_j^*}{P_j^3} \right), \quad (\text{A8})$$

$$-S_3 = \sum \left(\frac{S_{3j}}{P_j} - \frac{3}{2} \frac{R_{2j} Q_j}{P_j^2} + \frac{1}{2} \frac{Q_j^3}{P_j^3} \right). \quad (\text{A9})$$

All sums are over the source galaxy index j . Note that in the absence of applied shear, and with a circularly symmetric PSF, there is no preferred direction in the \mathbf{e} plane, and the expectation value of Q, R_2, S_1 , and S_3 are all zero. Only R_0 , therefore, remains finite in this limit. The other sums will be at most $O(g)$, although we will retain all terms in case the PSF can break the symmetry of the unsheared observations.

The posterior (A4) is simpler if we rotate to the frame where R_2 is real and the covariance matrix is diagonal. If the original R_2 has phase 2ϕ , then we set

$$\begin{aligned} \tilde{g} &= g e^{-i\phi} \equiv x + iy & (\text{A10}) \\ \tilde{Q} &= Q e^{-i\phi} \equiv Q_x + iQ_y \\ \tilde{S}_1 &= S_1 e^{-i\phi} \equiv S_{1x} + iS_{1y} \\ \tilde{S}_3 &= S_3 e^{-3i\phi} \equiv S_{3x} + iS_{3y} \\ \sigma_x^2 &= (R_0 + |R_2|)^{-1} \\ \sigma_y^2 &= (R_0 - |R_2|)^{-1}. \end{aligned}$$

As an aside, we note that if the measurement process (including PSF) has no preferred direction, then the applied shear \mathbf{g} sets the only axis of the system (which is ϕ), and a consequence will be that $\langle \tilde{Q} \rangle = \langle \tilde{S}_1 \rangle = \langle \tilde{S}_3 \rangle = 0$.

At quadratic order, (A4) implies a Gaussian posterior distribution in \mathbf{g} with both maximum and mean at

$$(x_0, y_0) = (-\sigma_x^2 Q_x, -\sigma_y^2 Q_y) = \left(\frac{-Q_x}{R_0 + |R_2|}, \frac{-Q_y}{R_0 - |R_2|} \right) \quad (\text{A11})$$

and independent errors on the components x and y of the shear in this rotated frame, equivalent to equations (7) and (6). We treat the cubic terms in (A4) as perturbations to the Gaussian

by assuming the $|S_{1,3}g^3| \ll 1$ at any g for which the Gaussian likelihood is significant. This approximation can be restated as

$$|SQ^3R_0^{-3}| \ll 1, \quad (\text{A12})$$

$$|SR_0^{-3/2}| \ll 1. \quad (\text{A13})$$

Under these conditions the posterior likelihood in the rotated \mathbf{g} frame can be expanded to first order in $S_{1,3}$ giving

$$P(\mathbf{g}|\mathbf{D}) \propto \exp\left[\frac{-(x-x_0)^2}{2\sigma_x^2}\right] \exp\left[\frac{-(y-y_0)^2}{2\sigma_y^2}\right] \left\{1 - \frac{1}{6}\text{Re}\left[\tilde{S}_1^*(x+iy) + \tilde{S}_3^*(x+iy)^3\right]\right\}. \quad (\text{A14})$$

The cubic term shifts the peak of the Gaussian posterior slightly, and adds some skew which shifts the expectation value further. The expectation value of shear under this posterior can be integrated to give

$$\begin{aligned} \langle x \rangle &= x_0 - \frac{S_{1x} + S_{3x}}{R_0 + |R_2|} \left(\frac{\sigma_x^2 + x_0^2}{2}\right) - \frac{S_{1x} - S_{3x}}{R_0 + |R_2|} \left(\frac{\sigma_y^2 + y_0^2}{6}\right) \\ &\quad - \frac{S_{1y} - 3S_{3y}}{R_0 + |R_2|} \left(\frac{x_0y_0}{3}\right) \\ \langle y \rangle &= y_0 - \frac{S_{1x} - 3S_{3x}}{R_0 - |R_2|} \left(\frac{x_0y_0}{3}\right) \\ &\quad - \frac{S_{1y} + S_{3y}}{R_0 - |R_2|} \left(\frac{\sigma_x^2 + x_0^2}{2}\right) - \frac{S_{1y} - S_{3y}}{R_0 - |R_2|} \left(\frac{\sigma_y^2 + y_0^2}{6}\right). \end{aligned} \quad (\text{A15})$$

In each case, the σ^2 terms in parentheses arise from the skewness imposed on $P(\mathbf{g}|\mathbf{D})$. Omitting them gives the location of the maximum of the posterior.

To obtain some understanding of this result, we take the case when the mean shear is determined to high accuracy, so the skewness becomes unimportant. Since we expect y_0, S_{1y} , and S_{3y} to be smaller than their x counterparts, and also $|R_2| \ll R_0$, the perturbation from cubic terms is expected to be dominated by a shift of the Gaussian likelihood to

$$\begin{aligned} \langle x \rangle &= \frac{-Q_x}{R_0 + |R_2|} - \frac{(S_{1x} + S_{3x})Q_x^2}{2(R_0 + |R_2|)^3} \\ \langle y \rangle &= \frac{-Q_y}{R_0 - |R_2|}. \end{aligned} \quad (\text{A16})$$

The main effect of the cubic term is therefore a slight shift of the shear posterior toward or away from the origin. We have not verified whether this abbreviated form is sufficiently accurate in cases with anisotropic PSFs, so the full form (A15) should be used.

To summarize, the procedure for estimating the shear using terms to 3rd order in g is:

1. From the unlensed ellipticity distribution P_0 and the shear transformation law, calculate the functions q, r_0, r_2, s_1 , and s_3 of e defined in equation (A1).
2. For each source galaxy j , integrate over e as per equations (A3) to obtain $P_j, Q_j, R_{0j}, R_{2j}, S_{1j}$, and S_{3j} .
3. Sum over source galaxies as per equations (A5)–(A9) to get Q, R_0, R_2, S_1 , and S_3 .
4. Rotate by the phase of R_2 to diagonalize the covariance matrix of the shear posterior and obtain transformed. Phases of the QRS components are changed and the shear component variances σ_x^2 and σ_y^2 are obtained as per equations (A10).
5. The maximum and mean of the quadratic solution in the rotated system are given by equations (A11).
6. The perturbation to the expectation value of the posterior due to cubic terms is in equations (A15).
7. Rotate back to original coordinate system.

B. Derivatives and transformations of the Fourier-domain moments

To implement the Bayesian Fourier-domain shear technique of Section 4, we need to calculate the first two derivatives of the moment vector in Equation (31) with respect to shear for each template galaxy. It is also helpful to know how these moments change under rotation, translation, and parity transformations, since the symmetries of the unlensed sky suggest that any template galaxy can be replicated with these transformations.

We start by writing the moments generally as

$$M_\alpha = \int d^2k \tilde{I}(\mathbf{k}) W(|\mathbf{k}^2|) F_\alpha(\mathbf{k}). \quad (\text{B1})$$

$\tilde{I}(\mathbf{k})$ is the Fourier transform of the pre-seeing galaxy image, and is related to the sky-plane surface brightness $I(\mathbf{x})$ by the usual

$$\tilde{I}(\mathbf{k}) = \int d^2x I(\mathbf{x}) \exp(i\mathbf{k} \cdot \mathbf{x}). \quad (\text{B2})$$

Consider a new galaxy image which is an affine transformation of the original image, specified by a linear amplification \mathbf{A} followed by translation by \mathbf{x}_0 :

$$I'(\mathbf{x}) = I(\mathbf{A}^{-1}\mathbf{x} - \mathbf{x}_0) \quad (\text{B3})$$

Standard Fourier manipulations give

$$\tilde{I}'(\mathbf{k}) = |\mathbf{A}| e^{i\mathbf{k}' \cdot \mathbf{x}_0} \tilde{I}(\mathbf{k}') \quad (\text{B4})$$

$$\mathbf{k}' \equiv \mathbf{A}^T \mathbf{k}. \quad (\text{B5})$$

The transformed moments are

$$M'_\alpha = |\mathbf{A}| \int d^2k \tilde{I}(\mathbf{k}') W(|\mathbf{k}'|^2) F_\alpha(\mathbf{k}) e^{i\mathbf{k}' \cdot \mathbf{x}_0} \quad (\text{B6})$$

$$= \int d^2k \tilde{I}(\mathbf{k}) W\left[\left|(\mathbf{A}^T)^{-1} \mathbf{k}\right|^2\right] F_\alpha\left[(\mathbf{A}^T)^{-1} \mathbf{k}\right] e^{i\mathbf{k} \cdot \mathbf{x}_0}. \quad (\text{B7})$$

B.1. Shear derivatives

We define a two-component shear $\mathbf{g} = (g_1, g_2)$ of a galaxy image with the flux-conserving transformation

$$\mathbf{A}^{-1} = \frac{1}{\sqrt{1-g^2}} \begin{pmatrix} 1+g_1 & g_2 \\ g_2 & 1-g_1 \end{pmatrix}. \quad (\text{B8})$$

It is convenient to adopt a complex notation at this point:

$$\begin{aligned} k &\equiv k_x + ik_y & \partial &\equiv \frac{\partial}{\partial g_1} - i \frac{\partial}{\partial g_2} \\ g &\equiv g_1 + ig_2 & \bar{\partial} &\equiv \frac{\partial}{\partial g_1} + i \frac{\partial}{\partial g_2} \end{aligned} \quad (\text{B9})$$

With this notation the action of shear $\mathbf{k} \rightarrow (\mathbf{A}^T)^{-1} \mathbf{k}$ becomes

$$k \rightarrow k' = (1 - g\bar{g})^{-1/2} (k + g\bar{k}). \quad (\text{B10})$$

Equation (B7) can now be restated in the complex notation for the case of a shear transformation:

$$M'_\alpha = \int d^2k \tilde{I}(k) W(k'\bar{k}') F_\alpha(k') \quad (\text{B11})$$

We are interested in the 2 scalar and 2 complex moments defined as

$$\begin{aligned} M_0 &= M_I & F_0 &= 1 \\ M_1 &= M_x + iM_y & F_1 &= ik \\ M_2 &= M_+ + iM_\times & F_2 &= k^2 \\ M_r & & F_r &= k\bar{k}. \end{aligned} \quad (\text{B12})$$

The shear derivative operators can be rewritten as

$$\nabla_g = \mathbf{v} \partial + \bar{\mathbf{v}} \bar{\partial} \quad \mathbf{v} \equiv \begin{pmatrix} 1 \\ i \end{pmatrix} \quad (\text{B13})$$

$$\nabla_g \nabla_g = \mathbf{v} \mathbf{v}^T \partial^2 + \bar{\mathbf{v}} \bar{\mathbf{v}}^T \bar{\partial}^2 + 2\mathbf{I}_2 \partial \bar{\partial} \quad \mathbf{I}_2 \equiv \begin{pmatrix} 1 & 0 \\ 0 & 1 \end{pmatrix} \quad (\text{B14})$$

Now the derivatives of the moments with respect to shear are obtained by applying these operators to the moment definition (B11) after substituting in the shear wavevector transformation (B10). For each moment, the derivatives can be expressed as

$$\nabla_g M_\alpha = \int d^2k \tilde{I}(k) [W(k\bar{k})A_\alpha(k) + W'(k\bar{k})B_\alpha(k)] \quad (\text{B15})$$

$$\nabla_g \nabla_g M_\alpha = \int d^2k \tilde{I}(k) [W(k\bar{k})C_\alpha(k) + W'(k\bar{k})D_\alpha(k) + W''(k\bar{k})E_\alpha(k)]. \quad (\text{B16})$$

Table 1 summarizes the results of propagating the shear derivatives into our weight and moment functions. All of the moments and their derivatives are simple weighted polynomial moments of the galaxy Fourier transform.

B.2. Rotation transformations

In our adopted complex notation, the effect of rotating the galaxy by angle ϕ is to send $k \rightarrow e^{i\phi}k$ in the argument of F_α in Equation (B7). The monopole moments M_0 and M_r are unchanged, while the dipole and quadrupole moments M_1 and M_2 acquire factors $e^{i\phi}$ and $e^{2i\phi}$, respectively. The rotational behavior of all the shear derivatives of the moments can also be easily assessed by applying the phase factors to all powers of k and \bar{k} in the elements of Table 1.

B.3. Parity transformations

A parity flip sends $k \leftrightarrow \bar{k}$ for all of the integrands of the moments and their derivatives in Table 1. The moments M_1 and M_2 are conjugated, meaning that M_y and M_x change sign, while the other moments are unchanged.

B.4. Derivatives with translation

A translation of the galaxy by \mathbf{x}_0 adds a factor $e^{i\mathbf{k}\cdot\mathbf{x}_0}$ to $\tilde{I}(\mathbf{k})$ in the integrand of all the moments (and their derivatives). In general the integrations of all the moments and their shear derivatives would need to be repeated.

We may, however, elect to approximate the effect of translation on the moments and their shear derivatives by linearizing about $\mathbf{x}_0 = 0$. In this case we are interested in $\frac{\partial M_\alpha}{\partial x_0}$, etc. The derivative of any moment or its derivatives with respect to x_0 can be obtained by adding a factor of $ik_x = i(k + \bar{k})/2$ to all the functions in Table 1. Similarly the y_0 derivative adds a factor $ik_y = (k - \bar{k})/2$ to the integrands.

If we adopt the linearization of the moments with translation, then for each template galaxy we need a substantial number of real-valued quantities: (6 moments) \times (1 moment + 5 derivatives)

for \mathbf{Q} and \mathbf{R}) \times (1 value + 2 translation derivatives) for a total of 108 numbers per template. The actual number of integrals we need to perform is much less than this since many elements are repeated in Table 1. Recall too that these template moments that define the prior only need to be evaluated once for the experiment, and the integrations are expressed as standard linear algebra routines. Evaluation of these quantities will not be a significant computational burden.

Table 1. Functional forms of the integrands for moments and their derivatives, as defined by Equations (B16). The derivatives of the moments under translate in x and y directions are found by adding factors of $i(k + \bar{k})/2$ and $(k - \bar{k})/2$ to the entries, respectively.

Moment	M_0	M_1	M_2	M_r
$F_\alpha =$	1	ik	k^2	$k\bar{k}$
$A_\alpha = \mathbf{v} \times$	0	$i\bar{k}$	$2k\bar{k}$	\bar{k}^2
$\quad + \bar{\mathbf{v}} \times$	0	0	0	k^2
$B_\alpha = \mathbf{v} \times$	\bar{k}^2	$ik\bar{k}^2$	$k^2\bar{k}^2$	$k\bar{k}^3$
$\quad + \bar{\mathbf{v}} \times$	k^2	ik^3	k^4	$k^3\bar{k}$
$C_\alpha = \mathbf{I}_2 \times$	0	ik	$2k^2$	$4k\bar{k}$
$\quad + \mathbf{v}\mathbf{v}^T \times$	0	0	$2\bar{k}^2$	0
$D_\alpha = \mathbf{I}_2 \times$	$4k\bar{k}$	$6ik^2\bar{k}$	$8k^3\bar{k}$	$8k^2\bar{k}^2$
$\quad + \mathbf{v}\mathbf{v}^T \times$	0	$2i\bar{k}^3$	$4k\bar{k}^3$	$2\bar{k}^4$
$\quad + \bar{\mathbf{v}}\bar{\mathbf{v}}^T \times$	0	0	0	$2k^4$
$E_\alpha = \mathbf{I}_2 \times$	$2k^2\bar{k}^2$	$2ik^3\bar{k}^2$	$2k^4\bar{k}^2$	$2k^3\bar{k}^3$
$\quad + \mathbf{v}\mathbf{v}^T \times$	\bar{k}^4	$ik\bar{k}^4$	$k^2\bar{k}^4$	$k\bar{k}^5$
$\quad + \bar{\mathbf{v}}\bar{\mathbf{v}}^T \times$	k^4	ik^5	k^6	$k^5\bar{k}$